An acid-stable β-glucosidase from Aspergillus aculeatus: Gene expression, biochemical characterization and molecular dynamics simulation

Yu Li, Xiaoyan Hu, Jingcheng Sang, Ying Zhang, Huitu Zhang, Fuping Lu, Fufeng Liu

PII: S0141-8130(18)32341-9
DOI: doi:10.1016/j.ijbiomac.2018.07.165
Reference: BIOMAC 10209

To appear in: *International Journal of Biological Macromolecules*

Received date: 15 May 2018
Revised date: 17 July 2018
Accepted date: 26 July 2018

Please cite this article as: Yu Li, Xiaoyan Hu, Jingcheng Sang, Ying Zhang, Huitu Zhang, Fuping Lu, Fufeng Liu , An acid-stable β-glucosidase from Aspergillus aculeatus: Gene expression, biochemical characterization and molecular dynamics simulation. Biomac (2018), doi:10.1016/j.ijbiomac.2018.07.165

An acid-stable β-glucosidase from *Aspergillus aculeatus*: Gene expression, biochemical characterization and molecular dynamics simulation

Yu Li[1,2,3,4], Xiaoyan Hu[4], Jingcheng Sang[4], Ying Zhang[4], Huitu Zhang[1,2,3,4], Fuping Lu[1,2,3,4*], Fufeng Liu[1,2,3,4*]

[1] State Key Laboratory of Food Nutrition and Safety (Tianjin University of Science & Technology), Tianjin, 300457, P. R. China;

[2] Tianjin Key Laboratory of Industrial Microbiology, Tianjin University of Science & Technology, Tianjin, 300457, P.R. China;

[3] National Engineering Laboratory for Industrial Enzymes, Tianjin, 300457, P.R. China;

[4] College of Biotechnology, Tianjin University of Science & Technology, Tianjin 300457, China.

Corresponding Authors

[*]F. Liu, Phone: +86-22-60602717; Fax: +86-22-60602298; E-mail: fufengliu@tust.edu.cn

[*]F. Lu, Phone: +86-22-60602271; Fax: +86-22-60602298; E-mail: lfp@tust.edu.cn

Abstract: β-Glucosidases hydrolyze terminal, non-reducing β-D-glucosyl residues and thereby release β-D-glucose. They have applications in the production of biofuels, beverages and pharmaceuticals. In this study, a β-glucosidase derived from *Aspergillus aculeatus* (BGLA) was expressed, characterized, and the molecular mechanism of its acid denaturation was comprehensively probed. BGLA exhibited maximal activity at pH 5.0–6.0. Its optimal temperature was 70 °C. Its enzyme activity was enhanced by Mg^{2+}, Ca^{2+} and Ba^{2+}, while Cu^{2+}, Mn^{2+}, Zn^{2+}, Fe^{2+} and Fe^{3+} had a negative effect. BGLA showed activity on a broad range of substrates including salicin, cellobiose, arbutin, geniposide and polydatin. Finally, the acid-denaturation mechanism of BGLA was probed using molecular dynamics (MD) simulations. The results of simulation at pH 2.0 imply that the contact number, solvent accessible surface area and number of hydrogen bonds in BGLA decreased greatly. Moreover, the distance between the residues Asp280 and Glu509 that are part of the active site increased, which eventually destroyed the enzyme's catalytic activity. These MD results explain the molecular mechanism of acid denaturation of BGLA, which will greatly benefit the rational design of more acid-stable β-glucosidase variants in the future.

Keywords: β-glucosidase, protein expression, molecular dynamics simulation, acid denaturation

1. Introduction

β-Glucosidases (BGLs) are a subgroup of β-D-glucoside glucohydrolases (EC 3.2.1.21). They were among the earliest discovered and widely studied enzymes due to their broad distribution and wide variety of substrates. BGLs are well characterized, biologically important enzymes that hydrolyze terminal, non-reducing β-D-glucosyl residues and thereby release β-D-glucose [1-3]. BGLs have attracted considerable attention due to their important roles in various biotechnological processes including the hydrolysis of pharmaceutical ingredients such as isoflavone glucosides [4-7], the production of fuel ethanol from agricultural residues [8-11], or the release of aromatic compounds from flavorless precursor [12-14]. Thus, BGLs have a great application value in the food, pharmaceutical and energy industries. Moreover, they are used in the wine-making process, which requires enzymes that can withstand low pH as well as high concentrations of ethanol or glucose [15, 16]. Since the beverage-making process is generally carried out under acidic conditions, and cellulose hydrolysis processes are routinely carried out at pH 4.5–5.0, acid-stable β-glucosidases have a wide range of industrial applications.

In addition to their use in industry, BGLs play pivotal roles in several biological processes. The physiological roles associated with these enzymes are diverse and depend on the location of the enzyme and the biological system in which they occur [17-19]. Filamentous fungi are known to be good β-glucosidase producers and a number of β-glucosidase were isolated from fungi [20-22]. However, reports on the cloning of BGLs from *Aspergillus aculeatus* are relatively rare, but enzymes from this

fungus are known to hydrolyze both soluble and insoluble cello-oligosaccharides [23], which makes them more widely applicable. Compared to BGLs from *Trichoderma reesei*, the BGL from *A. aculeatus* displays higher stability and conversion of sugars to ethanol [24]. Therefore, development of β-glucosidase from *A. aculeatus* has great significance.

Due to its exceptionally high extracellular protein production capacity, *Pichia pastoris* is an ideal gene expression system for heterologous protein expression, and it has been exploited for industrial enzyme production [25]. In this study, the gene encoding a β-D-glucosidase from *A. aculeatus* (BGLA; GenBank: D64088) was obtained from the NCBI database (https://www.ncbi.nlm.nih.gov/). The BGLA gene was optimized according to the codon usage of *P. pastoris* and synthesized. The codon-optimized gene was cloned into the pPIC9K vector and integrated into the *P. pastoris* strain GS115 by electroporation to achieve secretory expression of the recombinant protein. Subsequently, the enzymatic properties, substrate specificity, and function were investigated. Finally, the molecular mechanism of acid-denaturation of BGLA was comprehensively studied using an all-atom molecular dynamics simulation. These data will hopefully contribute to future industrial applications of this promising enzyme.

2. Materials and methods

2.1 Chemicals and reagents

Yeast extract and tryptone were purchased from Oxoid Ltd (Basingstoke, UK). DNA modifying enzymes and restriction enzymes were purchased from TaKaRa (Dalian, China). Salicin was purchased from Aladdin Bio-Chem Technology Co., LTD (Shanghai, China). Cellobiose, arbutin and geniposide were purchased from Solarbio Science & Technology Co., Ltd (Beijing, China). All other chemicals and reagents were of analytical grade and purchased from local sources.

2.2 Strains, media, and culture conditions

E. coli JM109, *P. pastoris* GS115, and the pPIC9K plasmids were all preserved in our laboratory. *E. coli* JM109 and *P. pastoris* GS115 were used as the host for gene cloning and expression of the target protein, respectively. *E. coli* JM109 was cultured in LB medium consisting of (g l^{-1}): tryptone, 10.0; yeast extract, 5.0; NaCl, 10.0; agar powder, 20.0 at 37 °C, and *P. pastoris* GS115 was culture in YPD medium consisting of (g l^{-1}): tryptone, 20.0; yeast extract, 10.0; glucose, 20.0; agar powder, 20.0 at 30 °C. For selection of transformants, the media were supplemented with the corresponding antibiotics.

2.3 Construction of plasmids for the overexpression of the putative β-glucosidase BGLA

We queried the NCBI database for β-D-glucosidase genes and found a DNA sequence containing an open reading frame with an intron encoding a putative BGLA gene. The sequence was optimized according to the preferences of *P. pastoris* (the preferences were provided in Table S1) and synthesized by GENEWIZ Co.,Ltd. Restriction endonuclease cutting sites for *Avr*II and *Not*I were incorporated into the 5'and 3' primer, respectively. The target gene was cloned into the pPIC9K vector and the vector was integrated into the genome of *P. pastoris* GS115 by electroporation to achieve secretory expression of recombinant β-glucosidase.

2.4 Expression, purification and de-glycosylation of BGLA

We picked single colony and placed the transformants into shaking tubes for enzyme production according to the protocol described in the *Pichia* manual (Invitrogen Life Technologies, Carlsbad, CA, USA). The cells were transferred to a sterile 50-ml centrifuge tube, centrifuged for 20 min at 4°C and 3000 × g, and the supernatant was collected. After passing through a 0.22 μm MCE filter, all of the enzyme purification steps were performed at 4°C. Ammonium sulfate was added to the filtrates containing BGLA under stirring to obtain 65% saturation for contaminant protein removal. The BGLA activities in the supernatants were recovered at 80% saturation. The precipitate formed was collected by centrifugation at 12,000 × g for 20 min and dissolved in 20 mM phosphate buffer (pH 6.6) and then dialyzed overnight at 4°C. Following ammonium sulfate precipitation, the BGLA dialysate was added to a

Toyopearl Super Q-650M column (1.6 × 4.0 cm, Tosoh Corp., Tokyo, Japan) which had been equilibrated with 20 mM phosphate buffer (pH 6.6). The column was washed with the same phosphate buffer and elution was then performed with a linear gradient of NaCl from 0 to 0.2 M in the same buffer. All of the eluted fractions were analyzed by SDS-PAGE. The activity of β-glucosidase was valuated using p-nitrophenyl-β-D-glucopyranoside (pNPG) as the substrate. The recombinant BGLA was subjected to de-glycosylation using PNGase F (New England Biolabs, Hitchin, UK) for 1 h at 37 °C following the manufacturer's instructions, prior to analysis by SDS-PAGE.

2.5 SDS-PAGE analysis and β-glucosidase activity assay

SDS-PAGE was performed using the method described by Laemmli [26]. β-Glucosidase activity was assayed using pNPG as the substrate. The reaction mixture, which consisted of 1.9 mL of citric acid/phosphate buffer (200 mM Na_2HPO_4 and 100 mM citric acid pH 5.0, the preparation of buffer was indicated in Table S1), 0.1 mL of enzyme sample and 1 mL of 3 mM pNPG, was incubated at 70 °C for 4 min. The reaction was terminated by adding 1 mL of 1 M Na_2CO_3. The absorbance of the released p-nitrophenol (pNP) was measured at 400 nm. One unit of enzyme activity was defined as the amount of enzyme that catalyzes the generation of l μmol of pNP per minute under the described assay conditions. Protein concentrations were determined using a BCA Protein Assay Kit with BSA as the standard. The enzyme activity was expressed as U/ml and the specific activity was expressed as U/mg.

2.6 Effect of temperature on the activity and stability of BGLA

The effect of temperature on the activity of BGLA was determined by incubating the enzyme at various temperatures ranging from 30 to 80°C in citric acid/phosphate buffer (200 mM Na_2HPO_4 and 100 mM citric acid, pH 5.0) using 3 mM pNPG as the substrate. The thermal stability of BGLA was examined by incubating the enzyme for 0.5 to 10 h at various temperatures (50, 60 and 70°C) in citric acid/phosphate buffer (200 mM Na_2HPO_4 and 100 mM citric acid, pH 5.0) without any substrate and after which the system was cooled to 37 °C before normal measurement of residual enzyme activity. In the test of the optimum temperature, the maximum activity obtained was defined as 100%. However, the initial activity was defined as 100% in the temperature stability study. All of the tests were repeated three times and the averages calculated.

2.7 Effect of pH on the activity and stability of BGLA

The effect of pH on the activity of BGLA was assessed in the pH range between 3.0 and 8.0 in citric acid/phosphate buffer (200 mM Na_2HPO_4 and 100 mM citric acid) at 70 °C. pH stability was determined by incubating the enzyme in buffers from pH 3.0 to 8.0 for 24 h at 4 °C, and valuating the remaining activity using the standard enzyme activity assay conditions. In the test of the optimum pH, the maximum activity obtained was defined as 100%. However, the initial activity was defined as 100% in the test of pH stability.

2.8 Effects of metal ions on the enzyme activity of BGLA

To investigate the effects of different metal ions on the enzyme activity of BGLA, various metal ions (Mg^{2+}, Ca^{2+}, Cu^{2+}, Mn^{2+}, Zn^{2+}, Fe^{2+}, Fe^{3+} and Ba^{2+}) were added individually into the reaction system with final concentrations of 1 mM, 5 mM or 10 mM. Enzyme solutions containing each individual metal ion at optimal pH and temperature (i.e. pH 5.0 and 70°C) were incubated with 3mM pNPG substrate for 4 min, and the enzyme activity was measured as described above. The activity in the sample without metal ions was taken as the positive control (100%).

2.9 Analysis of substrate specificity

For substrate specificity analyses, pNPG, salicin, cellobiose, arbutin, geniposide and polydatin were tested. β-Glucosidase catalyzes the hydrolysis of β-glucosidic linkages of various glycosides to form glucose and an aglycone. Accordingly, the enzymatic activity was measured by detecting the product formation and expressed as U/mg. One unit (U) was defined as the amount of enzyme that releases l μmol of glucose or aglycone per minute under the described assay conditions. Detailed information on the substrates including chemical structure and their corresponding aglycones is listed in Table S8. The activities toward natural substrates (e.g., salicin, cellobiose arbutin and geniposide) were determined by measuring the amount of released glucose. The activity toward polydatin was determined by measuring the resveratrol. The target enzyme BGLA was mixed with each of the 2 mM substrates and incubated for 20 min at 70 °C. The reaction was stopped by boiling for 10 min,

and the amount of product was measured by HPLC. The HPLC was conducted using a Prevail Carbohydrate ES 5u column (250mm×4.6mm, Agilent, USA) toward the detection of glucose, and using a Zorbax-C18 column (Agilent, USA) to detected the resveratrol.

2.10 Molecular dynamics simulation

All MD simulations were carried out using the GROMACS 5.1.2 software package, together with GROMOS 53A6 force field parameters [27]. The 3D structure of β-glucosidase from *A. aculeatus* resolved at 1.8 Å (PDB ID: 4IIB) was used as the initial structure [28]. The detailed simulation parameters were the same as described elsewhere [29, 30]. Briefly, the protein was first solvated into a cubic box with an edge length of 97 Å. The SPC water model was used to represent water. Following similar protocols as used in our previous studies[31-34]. The simulation systems were first relaxed with 5000 steps of conjugate gradient minimization to avoid any unacceptable contacts between the protein and water molecules. The simulation system was first equilibrated for 200 ps under an isochoric-isothermal (NVT) ensemble using the Berendsen weak coupling method [35]. It was further equilibrated for 200 ps under an isothermal-isobaric (NPT) ensemble using the same method. Position restraints were applied to BGLA during the entire equilibration process. Finally, production MD simulations were performed using the NPT ensemble without any restraints. Temperature (300 K) and pressure (1 atm) were regulated by the Nosé-Hoover thermostat [36] and Parrinello-Rahman barostat [37], respectively. To

ensure that the effect of pH on the conformational stability of BGLA is intrinsic to the protein rather than a stochastic output of the simulations, three MD simulations of 50 ns were conducted for each system under different initial conditions by assigning different initial velocities to each atom of the simulation systems. Table S9 summarizes the important data for the different simulated systems.

The particle-mesh Ewald method was used to process the long-ranged electrostatic interactions [38]. The short-ranged van der Waals interactions were processed with a cutoff of 10 Å. The LINCS algorithm was used to limit the bond length of the protein [39], and the SETTLE algorithm[40] was used to constrain the water bond lengths and angles. Periodic boundary conditions were applied for all three directions. To make sure that the effects of pH on protein stability reflect the intrinsic character rather than a stochastic output of the simulation, three independent 50-ns-long simulation trajectories were collected for data analysis.

In order to mimic the environment of the two pH values (i.e., 2.0 and 5.0), the side-chains of the negatively charged Glu and Asp residues were modified to have different charge states based on their isoelectric points. At pH 2.0, both Asp and Glu are neutral, while at pH 5.0, they are negatively charged. By contrast, the charged residues of Arg, Lys and His are positively charged, and the other residues are neutral. The same strategy was often applied in MD simulations to investigate pH-dependent protein folding/aggregation [41-43]. Thus, the environmental pH was accounted for by choosing the charge states of the described relevant residues in our MD simulations.

The simulation trajectories were analyzed using several auxiliary programs provided with the GROMACS 5.1.2 package. The values of the root-mean-square deviation of Cα atoms (Cα-RMSD), radius of gyration (Rg), root mean square fluctuation (RMSF), the number and distances of contacts, solvent accessible surface area (SASA), and hydrogen bonds (H-bonds) were calculated using *gmx rms*, *gmx gyrate*, *gmx rmsf*, *gmx mindist*, *gmx sasa and gmx hbond* programs, respectively. VMD software version 1.9.3 (http://www.ks.uiuc.edu/Research/vmd/) was used for the visualization and analysis of molecules and trajectories [44].

3. Results and discussion

3.1 Expression and purification of BGLA from *A. aculeatus*

The sequence of the BGLA gene from *A. aculeatus* was obtained by searching the NCBI database. The target gene was codon optimized, synthesized, cloned into the pPIC9K vector and overexpressed in *P. pastoris* GS115. The recombinant β-glucosidase was purified from the culture filtrates of the *P. pastoris* GS115 transformants that overexpressed the *bglA* gene. The protein from the culture filtrate was concentrated and a dialyzed enzyme solution was obtained. BGLA was purified from the crude enzyme solution by anion exchange chromatography.

The purification of BGLA is summarized in Table 1 and the purified protein was analyzed by SDS-PAGE. As shown in Fig. 1, a single band on the SDS-PAGE gel was observed with an apparent molecular mass of ~130 kDa. The full-length cDNA of the *bglA* gene consisted of 2583 base pairs that encode a polypeptide of 860 amino acids.

The theoretical molecular mass and isoelectric point (pI) were 93.05 kDa and 5.03, respectively. Hence, the apparent molecular mass (~130 kDa) of the purified BGLA was much higher than the theoretical value (93.05 kDa). This discrepancy may be caused by glycosylation, which is commonly observed when *P. pastoris* is used to secret target proteins into the extracellular space [45]. It should be kept in mind that correct glycosylation and folding is sometimes necessary to ensure the biological activity of recombinant proteins [46, 47]. After treatment with PNGase F, the protein band of BGLA was similar to the expected one. Moreover, the molecular weight of BGLA was confirmed by matrix-assisted laser desorption/ionization time of flight mass spectrometry (MALDI-TOF) (Fig. S1), and the result was consistent with the SDS-PAGE results.

Finally, the standard assay mixture with pH 5.0 was used for the determination of β-glucosidases activity. The specific activity was 281.0 U/mg, which was higher than the specific activity of two published β-glucosidases from *Aspergillus fumigatus* Z5, at 103.5 and 101.7 U/mg [48].

3.2 Effects of temperature and pH on the activity and stability of BGLA

It is known that temperature and pH greatly affect the enzymatic activity of β-glucosidases [49-52]. We examined the effects of temperature on the activity and stability of BGLA. The results have shown that BGLA can maintain more than 60% relative activity between 50-75°C, and the optimal temperature was 70°C (Fig. 2A),

which was higher than the optimum temperature of the enzyme from *A. fumigatus* Z5 [48]. The thermostability was also assessed as shown in Fig. 2B. The raw data are shown in Tables S3-S4. BGLA showed high thermostability at 50°C, retaining more than 89% relative activity after 10 h. However, at 60 and 70°C, the enzyme was significantly less stable. Nevertheless, it still maintained more than 50% activity after 2 h at these temperatures. Taken together, the results show that BGLA has good thermostability, which gives it a wider range of potential applications than other β-glucosidases, which is more conducive to the reactions in industrial production and some conversion processes [2, 53].

The enzyme displayed more than 60% activity at pH values between 4.5 and 6.0 with a pH optimum of 5.0 (Fig.2C). Moreover, BGLA was very stable in the pH range of 3.0–8.0, where it maintained more than 40% relative activity after pre-incubation for 24 h (Fig.2D). The raw data are shown in Tables S5 and S6. Overall, the enzyme showed maximum activity at pH 5.0, which was lower than the optimum pH of the β-glucosidase from *A. fumigatus* (pH 6.0) [48]. However, β-glucosidases from *A. niger* showed the same pH optimum [54]. Therefore, BGLA is a moderately acid-stable β-glucosidase, which indicates that it has good potential for application in cellulose hydrolysis processes, which are routinely carried out at pH 4.0–5.0 [55-57]. Furthermore, the pH stability of BGLA was superior to that of the β-glucosidase from *Dekkera bruxellensis* (teleomorph of *Brettanomyces*)[58], which makes it suitable for a wider range of applications under low-pH conditions, including fruit and vegetable processing in beverage production, as well as cellulose hydrolysis [57]. While the pH

tolerance and stability of β-glucosidases from different microbial species are generally variable, and most of them prefer the acidic pH range [59-61], several β-glucosidases displayed a broad range of pH stability that indicated their potential suitability for a wide range of industrial processes. These enzymes were stable at pH 3.0~7.0 [62], which was similar to the experimental observations from this study.

3.3. Effects of metal ions on the activity of BGLA

The effects of different metal ions on the activity of BGLA were investigated using assays with the addition of metal ions (1 mM, 5 mM or 10 mM) in conjunction with pNPG as substrate. This information is important because many ions are ubiquitously present in various biotechnological processes that utilize β-glucosidases. Fig. 3 shows the effects of various metal ions on the activity of BGLA (the raw data are shown in Table S7). Mg^{2+}, Ca^{2+} and Ba^{2+} greatly increased the enzymatic activity of BGLA, which was higher by more than 119.8, 126.0 and 112.7% in their presence, respectively. By contrast, Cu^{2+}, Mn^{2+}, Zn^{2+}, Fe^{2+} and Fe^{3+} inhibited the enzymatic activity (Fig. 3), whereby Fe^{2+} greatly decreased the enzyme activity down to 55.8%. Similarly, the β-glucosidase from *Sclerotinia sclerotiorum* was reported to be inhibited by Fe^{2+}, which reduced the activity down to 1.2% [63].

3.4. Substrate specificity of BGLA

A variety of artificial and natural substrates were employed in the substrate specificity analysis of recombinant BGLA (Table 2). The enzyme showed a certain hydrolytic activity towards pNPG, salicin, cellobiose, arbutin, geniposide and

polydatin. The enzyme had its highest activity with pNPG (73.56 ± 0.87 U/mg). The most preferred natural substrate was arbutin, which was similar to the substrate preference of β-glucosidase from *A. oryzae* [64]. Furthermore, BGLA had better specificity for arbutin (12.97 ± 0.59 U/mg) and salicin (7.40 ± 0.23 U/mg) than cellobiose (6.50 ± 0.30 U/mg). The β-glucosidase from *A. oryzae* also showed better specificity for arbutin than cellobiose [65]. Thus, BGLA may be specific for aryl β-glucosides (arbutin and salicin) to some extent. Overall, these results indicate that the recombinant β-glucosidase has a reasonably broad substrate spectrum.

3.5 Molecular mechanism of the acid denaturation of BGLA probed by molecular dynamics simulations

Based on the preceding experimental data, it was clear that BGLA showed excellent acid-tolerance, with an optimal pH for activity of 5.0. However, very low activity was observed at pH 2.0. Therefore, it was important to probe the molecular mechanism of protein stability of BGLA at different pH values, since this knowledge can benefit the rational design of β-glucosidase with a higher tolerance to low pH. Therefore, all-atom MD simulations were carried out to better understand the molecular mechanism of protein stability of BGLA at low pH values. To this end, three independent rounds of simulation spanning 50 ns were performed as described in previous methods. First, two structural parameters, the RMSD from the initial structure for Cα atoms and the Rg of the whole BGLA, were used to represent the structural stability of the protein. The values of Cα-RMSD and Rg are displayed as a

function of simulation time in Figs. 4A and B, respectively. As can be seen in Fig. 4A, after a rapid increase during the initial 1 ns, the Cα-RMSD values at pH 2.0 were larger than those at pH 5.0 during most of the simulation time. For example, the Rg value of BGLA at pH 2.0 increased greatly to 2.88 nm during the initial 1 ns, which was larger than at pH 5.0 (Fig. 4B). A similar phenomenon was also observed for the values of Rg. Another structural parameter, Rg, was also used to assess the compactness of the proteins during the MD simulation. Therefore, BGLA can be considered stable at pH 5.0 based on the results of the MD simulation, which was consistent with the experimental results (Fig. 2C).

To probe the effect of pH on the protein stability of BGLA, two further structural parameters, SASA and inter-residue contact number, were also calculated (Fig. 5). As can be seen, at pH 5.0, the value of SASA remained stable around 335 nm^2 during the entire MD simulation. By contrast, at pH 2.0, SASA increased greatly to above 360 nm^2. At the same time, the contact number of BGLA decreased greatly at pH 2.0. Moreover, the intra-molecular hydrogen bonds were also calculated and displayed as a function of time in Fig. 5C. At pH 5.0, the number of the intra-molecular hydrogen bonds of BGLA was about 530, which was more than at pH 2.0. Representative snapshots of the BGLA at different pH values are shown in Fig. 7. Therefore, the overall structure of BGLA was less compact at pH 2.0, and hence the number of intra-molecular hydrogen bonds was decreased.

The RMSF is commonly used to represent the positional fluctuations of residues during the MD simulation process. Fig. 6 shows the RMSF values as a function of

amino acid sequence at pH 2.0 and 5.0 during the 50-ns MD simulation. As can be seen in Fig. 6, the RMSF values of the region of 720-748 and 280-285 varied much more at pH 2.0 than at 5.0. The locations of these residues in BGLA and their corresponding secondary structures are shown in Fig. S2. The fluctuating residues mainly formed bend and random coil structures, and the region of 720-748 was expanded and exposed to the solvent, so that it interacted with few residues from other regions of the protein. Therefore, this region is greatly affected by the acidic environment and the RMSF value fluctuates greatly. Moreover, the residue Glu280 in the active site of BGLA located in the region of 280-285 was also susceptible to the simulated acidic environment.

The two residues Asp280 and Glu509 constitute the active site of BGLA [1, 66]. In order to further probe the exact locations of these two residues, their mutual distances were calculated as shown in Fig. 9. The distance between the residues Asp280 and Glu509 was clearly larger at pH 2.0 than at pH 5.0 (Fig. 8). It was about 9 Å at pH 5.0, which is similar to the distance in the native state, while it was more than 15 Å at pH 2.0. Typical snapshots of the two active-site residues are shown in Fig. 9. The change of the distance between Asp280 and Glu509 is most likely caused by the general loss of compactness of BGLA's overall structure (Figs. 4B and 5B), which may result in great structural fluctuation, a reduced number of contacts among residues and a reduced number of hydrogen bonds (Figs. 5A, 5C and 6). Based on the molecular mechanism of acid-induced denaturation of BGLA probed by molecular dynamics simulations, we revealed the decrease of contact number, SASA and the

number of the hydrogen bonds in BGLA, which will greatly benefit the rational design of new enzymes with improved acid stability. For example, inhibition of the structural expansion and enhancement of hydrogen bonds among the residues of the target proteins would enable the rational design of a novel β-glucosidase that is well adapted to acidic conditions.

4. Conclusions

In this study, we discovered and characterized a β-glucosidase from *Aspergillus aculeatus*, which was named BGLA. The enzyme was heterologously expressed, purified, and biochemically characterized. Recombinant BGLA exhibited maximal enzymatic activity at pH 5.0-6.0 and its optimal temperature was 70°C. BGLA displayed activity with a broad array of substrates, including salicin, cellobiose, arbutin, geniposide and polydatin. Moreover, the molecular mechanism of the acid stability of BGLA was investigated using all-atom molecular dynamics simulations. The contact number, SASA and number of hydrogen bonds of BGLA decreased greatly during the MD simulation. Hence, the protein's intra-molecular interactions were weakened at low pH, so that the distance between the active-site residues Asp280 and Glu509 increased greatly. Consequently, the catalytic activity of BGLA was completely destroyed at pH 2.0. This study thus reveals the molecular mechanism of acid-tolerance of BGLA, which will hopefully inspire the rational design of more acid-tolerant industrial enzymes in the future.

Acknowledgements

This work was funded by the National Natural Science Foundation of China (No. 21576199) and the Natural Science Foundation of Tianjin from the Tianjin Municipal Science and Technology Commission (Contract No. 18JCZDJC33000).

Conflicts of interest

The authors declare no conflicts of interest.

References

[1] J.C. Ketudat, A. Esen, β-Glucosidases, Cel. Mol. Life Sci. 67 (2010) 3389-3405.

[2] Y. Bhatia, S. Mishra, V.S. Bisaria, Microbial β-Glucosidases: Cloning, Properties, and Applications, Crit. Rev. Biotechnol. 22 (2008) 375-407.

[3] J.R.K. Cairns, B. Mahong, S. Baiya, J.-S. Jeon, β-Glucosidases: Multitasking, moonlighting or simply misunderstood?, Plant Sci. 241 (2015) 246-259.

[4] B.N. Kim, S.J. Yeom, Y.S. Kim, D.K. Oh, Characterization of a β-glucosidase from *Sulfolobus solfataricus* for isoflavone glycosides, Biotechnol. Lett. 34 (2012) 125-129.

[5] J. Xiao, T.S. Muzashvili, M.I. Georgiev, Advances in the biotechnological glycosylation of valuable flavonoids, Biotechnol Adv 32 (2014) 1145-1156.

[6] B. EunAh, P. SunYoung, K. DongHyun, Constitutive β-glucosidases hydrolyzing ginsenoside Rb1 and Rb2 from human intestinal bacteria, Biol. Pharm Bull. 23 (2000) 1481-1485.

[7] R.I. Tennen, E. Michishitakioi, K.F. Chua, Finding a target for resveratrol, Cell 148 (2012) 387-389.

[8] E.S. Lymar, B. Li, V. Renganathan, Purification and Characterization of a Cellulose-Binding (beta)-Glucosidase from Cellulose-Degrading Cultures of *Phanerochaete chrysosporium*, Appl Environ Microbiol. 61 (1995) 2976-2980.

[9] L. Zhao, Q. Pang, J. Xie, J. Pei, F. Wang, S. Fan, Enzymatic properties of Thermoanaerobacterium thermosaccharolyticum β-glucosidase fused to Clostridium cellulovorans cellulose binding domain and its application in hydrolysis of microcrystalline cellulose, BMC Biotechnol. 13 (2013) 101.

[10] R.R. Singhania, A.K. Patel, A. Pandey, E. Ganansounou, Genetic modification: A tool for enhancing beta-glucosidase production for biofuel application, Bioresour. Technol. 241 (2017) 309.

[11] M. Dcb, C. Leite, S. Lhs, L.F. Marins, K.S. Machado, A.V. Werhli, L. Lhf, R.C. de MeloMinardi, Characterization of glucose-tolerant β-glucosidases used in biofuel production under the bioinformatics perspective: a systematic review, Genetics and Molecular Research .16 (2017).

[12] Y. Wang, C. Zhang, J. Li, Y. Xu, Different influences of β-glucosidases on volatile compounds and anthocyanins of Cabernet Gernischt and possible reason, Food Chem.140 (2013) 245-254.

[13] S.E. Tokpohozin, S. Fischer, B. Sacher, T. Becker, β-d-Glucosidase as "key enzyme" for sorghum cyanogenic glucoside (dhurrin) removal and beer bioflavouring, Food Chem Toxicol. 97 (2016) 217-223.

[14] J.M. Almeida, V.A. Lima, P.C. Giloni-Lima, A. Knob, Passion fruit peel as novel substrate for enhanced β-glucosidases production by Penicillium verruculosum : Potential of the crude extract for biomass hydrolysis, Biomass Bioenergy. 72 (2015) 216-226.

[15] P. González-Pombo, L. Fariña, F. Carrau, F. Batista-Viera, B.M. Brena, A novel extracellular β-glucosidase from Issatchenkia terricola: Isolation, immobilization and application for aroma enhancement of white Muscat wine, Process Biochemistry 46 (2011) 385-389.

[16] R.N. Barbagallo, G. Spagna, R. Palmeri, C. Restuccia, P. Giudici, Selection, characterization and comparison of β-glucosidase from mould and yeasts employable for enological applications, Enzyme Microbl Technol. 35 (2004) 58-66.

[17] R.R. Singhania, A.K. Patel, R.K. Sukumaran, C. Larroche, A. Pandey, Role and significance of beta-glucosidases in the hydrolysis of cellulose for bioethanol production, Biores. Technol. 127 (2013) 500-507.

[18] W.Y. Jeng, N.C. Wang, M.H. Lin, C.T. Lin, Y.C. Liaw, W.J. Chang, C.I. Liu, P.H. Liang, A.H. Wang, Structural and functional analysis of three β-glucosidases from bacterium *Clostridium cellulovorans*, fungus *Trichoderma reesei* and termite *Neotermes koshunensis*, J Struct Biol.173 (2011) 46-56.

[19] R.Z. Ventorim, D.O.M. Ta, L.M. Trevizano, D.S.C. Am, V.M. Guimarães, Impact of the removal of N-terminal non-structured amino acids on activity and stability of xylanases from *Opinomyces sp.* PC-2, Int J Biol Macromol. S0141-8130（17）31425-3.

[20] G. Molina, F.J. Contesini, R.R.D. Melo, H.H. Sato, G.M. Pastore, β-Glucosidase From *Aspergillus*, In: New and future developments in microbial biotechnology and bioengineering, 2016, pp 155–169..

[21] Z. Wen, L. Wei, S. Chen, Production of cellulase/β-glucosidase by the mixed fungi culture *Trichoderma reesei* and *Aspergillus phoenicis* on dairy manure, Process Biochem. 121 (2005) 93.

[22] F. Bhiri, S.E. Chaabouni, F. Limam, R. Ghrir, N. Marzouki, Purification and Biochemical Characterization of Extracellular β-Glucosidases from the Hypercellulolytic Pol6 Mutant of *Penicillium occitanis*, Appl Biochem Biotechnol. 149 (2008) 169-182.

[23] J. Ito, T. Ebe, S. Shibasaki, H. Fukuda, A. Kondo, Production of alkyl glucoside from cellooligosaccharides using yeast strains displaying *Aspergillus aculeatus* β-glucosidase 1, J. Mol. Catal. B Enzym. 49 (2007) 92-97.

[24] T. Treebupachatsakul, H. Nakazawa, H. Shinbo, H. Fujikawa, A. Nagaiwa, N. Ochiai, T. Kawaguchi, M. Nikaido, K. Totani, K. Shioya, Heterologously expressed *Aspergillus aculeatus*

β-glucosidase in *Saccharomyces cerevisiae* is a cost-effective alternative to commercial supplementation of β-glucosidase in industrial ethanol production using Trichoderma reesei cellulases, J. Biosci. Bioeng. 121 (2016) 27-35.

[25] O. Cos, A. Serrano, J.L. Montesinos, P. Ferrer, J.M. Cregg, F. Valero, Combined effect of the methanol utilization (Mut) phenotype and gene dosage on recombinant protein production in *Pichia pastoris* fed-batch cultures, J. Biotechnol. 116 (2005) 321-335.

[26] U.K. Laemmli, Cleavage of Structural Proteins during the Assembly of the Head of Bacteriophage T4, Nature 227(5259) (1970) 680-685.

[27] L. Pol-Fachin, H. Verli, R.D. Lins, Extension and Validation of the GROMOS 53A6(GLYC) Parameter Set for Glycoproteins, J Comput Chem. 35 (2014) 2087-2095.

[28] K. Suzuki, J. Sumitani, Y.W. Nam, T. Nishimaki, S. Tani, T. Wakagi, T. Kawaguchi, S. Fushinobu, Crystal structures of glycoside hydrolase family 3 beta-glucosidase 1 from *Aspergillus aculeatus*, Biochem J 452 (2013) 211-221.

[29] F.F. Liu, X.Y. Dong, L. He, A.P. Middelberg, Y. Sun, Molecular insight into conformational transition of amyloid beta-peptide 42 inhibited by (-)-epigallocatechin-3-gallate probed by molecular simulations, J Phys Chem B. 115 (2011) 11879-11887.

[30] F.F. Liu, L. Ji, L. Zhang, X.Y. Dong, Y. Sun, Molecular basis for polyol-induced protein stability revealed by molecular dynamics simulations, J Chem Phys. 132 (2010) 225103-225109.

[31] N. Zhang, F.F. Liu, X.Y. Dong, Y. Sun, Molecular Insight into the Counteraction of Trehalose on Urea-Induced Protein Denaturation Using Molecular Dynamics Simulation, J Phys Chem B. 116 (2012) 7040-7047.

[32] Y. Tu, S. Ma, F. Liu, Y. Sun, X. Dong, Hematoxylin Inhibits Amyloid β-Protein Fibrillation and Alleviates Amyloid-Induced Cytotoxicity, J Phys Chem B. 120 (2016).

[33] J. Guo, W. Sun, L. Li, F. Liu, W. Lu, Brazilin inhibits fibrillogenesis of human islet amyloid polypeptide, disassembles mature fibrils, and alleviates cytotoxicity, Rsc Advances. 7 (2017) 43491-43501.

[34] W.J. Du, J.J. Guo, M.T. Gao, S.Q. Hu, X.Y. Dong, Y.F. Han, F.F. Liu, S. Jiang, Y. Sun, Brazilin inhibits amyloid β-protein fibrillogenesis, remodels amyloid fibrils and reduces amyloid cytotoxicity, Sci. Rep. 5 (2015) 7992.

[35] H.J.C. Berendsen, J.P.M. Postma, W.F.V. Gunsteren, A. Dinola, J.R. Haak, Molecular dynamics with coupling to an external bath, J. Chem. Phys. 81 (1984) 3684-3690.

[36] W.G. Hoover, Canonical dynamics: Equilibrium phase-space distributions, Physical Review A 31 (1985) 1695-1697.

[37] S. Nosé, M.L. Klein, A study of solid and liquid carbon tetrafluoride using the constant pressure molecular dynamics technique, J.Chem.Phys. 78(11) (1983) 6928-6939.

[38] U. Essman, L. Perera, M.L. Berkowitz, T. Darden, H. Lee, L.G. Pedersen, A smooth particle mesh Ewald method, J Chem Phys. 103 (1995) 8577-8593.

[39] B. Hess, H. Bekker, H.J.C. Berendsen, J.G.E.M. Fraaije, LINCS: A linear constraint solver for molecular simulations, J Comput Chem 18 (1997) 1463-1472.

[40] S. Miyamoto, P.A. Kollman, Settle: An analytical version of the SHAKE and RATTLE algorithm for rigid water models, Journal of Computational Chemistry 13 (1992) 952–962.

[41] B.A. Narendra, R.M. Kumar, R.V. Hosur, Visualization of Early Events in Acetic Acid Denaturation of HIV-1 Protease: A Molecular Dynamics Study, Plos One 6(6) (2011) e19830.

[42] Y. Li, W. Xu, Y. Mu, J.Z. Zhang, Acidic pH retards the fibrillization of human Islet Amyloid Polypeptide due to electrostatic repulsion of histidines, J. Chem. Phys. 139 (2013) 055102.

[43] J. Wang, Y. Zhang, X. Wang, J. Shang, Y. Li, H. Zhang, F. Lu, F. Liu, Biochemical characterization and molecular mechanism of acid denaturation of a novel α-amylase from Aspergillus niger, Biochem Eng J. 137 (2018) 222-231.

[44] W. Humphrey, A. Dalke, K. Schulten, VMD: Visual molecular dynamics, J Mol Graph Model 14 (1996) 33-38.

[45] J.M. Cregg, J.L. Cereghino, J. Shi, D.R. Higgins, Recombinant protein expression in *Pichia pastoris*, Molecular Biotechnology 16 (2000) 23-52.

[46] R.K. Bretthauer, F.J. Castellino, Glycosylation of Pichia pastoris-derived proteins, Biotechnol Appl Biochem 30 (1999) 193-200.

[47] M. Lagzian, A. Shahraki, M. Besharatian, A. Asoodeh, A thermostable alkaliphilic protein-disulfide isomerase from Bacillus subtilis DR8806: cloning, expression, biochemical characterization and molecular dynamics simulation, Int J Bio Macromol. (2017) 703-712.

[48] D. Liu, R. Zhang, X. Yang, Z. Zhang, S. Song, Y. Miao, Q. Shen, Characterization of a thermostable β-glucosidase from Aspergillus fumigatus Z5, and its functional expression in *Pichia pastoris* X33, Microb. Cell Fact. 11 (2012) 25.

[49] S. Nataraja, D.M. Chetan, M. Krishnappa, Effect of temperature on cellulose enzyme activity in crude extracts isolated from solid wastes microbes, Int J Microbiol Res. 2 (2010) 44-47.

[50] R.M. Daniel, M.J. Danson, R. Eisenthal, C.K. Lee, M.E. Peterson, The effect of temperature on enzyme activity: new insights and their implications, Extremophiles 12 (2008) 51-59.

[51] G. Szasz, The effect of temperature on enzyme activity and on the affinity of enzymes to their substrates, Z. Klin. Chem. Klin. Biochem. 12 (1974) 166-170.

[52] W.B. Neely, Studies on the Enzyme Dextransucrase. I. The Effect of pH on Enzyme Activity, J. Am. Chem. Soc. 80 (1958) 2010-2013.

[53] X. Yang, R. Ma, P. Shi, H. Huang, Y. Bai, Y. Wang, P. Yang, Y. Fan, B. Yao, Molecular Characterization of a Highly-Active Thermophilic β-Glucosidase from *Neosartorya fischeri* P1 and Its Application in the Hydrolysis of Soybean Isoflavone Glycosides, Plos One. 9 (2014) e106785-e106785.

[54] F.Y. Yan, W. Xia, X.X. Zhang, S. Chen, X.Z. Nie, L.C. Qian, Characterization of β-glucosidase from *Aspergillus terreus* and its application in the hydrolysis of soybean isoflavones, J. Zhejiang Univ. Sci. B. 17 (2016) 455-464.

[55] M. Sohail, R. Siddiqi, A. Ahmad, S.A. Khan, Cellulase production from *Aspergillus niger* MS82: effect of temperature and pH, New Biotechnology. 25 (2009) 437-441.

[56] J.P.H.V. Wyk, Cellulase catalyzed hydrolysis of cellulose materials: PH and temperature profiles, Resource Environ. Biotechnol. 2 (1999) 249-254.

[57] L.T. Fan, M.M. Gharpuray, Y.H. Lee, Cellulose Hydrolysis, Springer Berlin Heidelberg. 3(1987) 1-68.

[58] H.P. Kuo, R. Wang, C.Y. Huang, J.T. Lai, Y.C. Lo, S.T. Huang, Characterization of an extracellular β-glucosidase from *Dekkera bruxellensis* for resveratrol production, J. Food Drug Anal. (2018) 163-171.

[59] J. Kaur, B.S. Chadha, B.A. Kumar, G. Kaur, S, H.S. Saini, Purification and characterization of ß-glucosidase from *Melanocarpus sp.* MTCC 3922, Electron J Biotechn. 10 (2007) 260-270.

[60] J.D. Kim, C.G. Lee, Purification and characterization of extracellular beta-glucosidase from *Sinorhizobium kostiense* AFK-13 and its algal lytic effect on Anabaena flos-aquae, Cardiologia 32 (1987) 1603.

[61] N.J. Parry, D.E. Beever, E. Owen, I. Vandenberghe, B.J. Van, M.K. Bhat, Biochemical characterization and mechanism of action of a thermostable beta-glucosidase purified from *Thermoascus aurantiacus*, Biochem J. 353 (2001) 117-127.

[62] C. Riou, J.M. Salmon, M.J. Vallier, Z. Günata, P. Barre, Purification, characterization, and substrate specificity of a novel highly glucose-tolerant beta-glucosidase from *Aspergillus oryzae*, Appl.environ.microbiol 64 (1998) 3607-14.

[63] S.M. Issam, G. Mohamed, L.M. Dominique, M. Thierry, L. Farid, M. Nejib, A β-glucosidase from *Sclerotinia sclerotiorum*, Appl Biochem Biotechnol. 112 (2004) 63-77.

[64] A. Watanabe, M. Suzuki, S. Ujiie, K. Gomi, Purification and enzymatic characterization of a novel β-1,6-glucosidase from *Aspergillus oryzae*, J. Biosci. Bioeng. 121 (2016) 259-264.

[65] K. Kanako, W. Akira, U. Seiryu, S. Takahiro, G. Katsuya, Purification and enzymatic characterization of secretory glycoside hydrolase family 3 (GH3) aryl β-glucosidases screened from *Aspergillus oryzae* genome, Journal of Bioscience & Bioengineering 120 (2015) 614-23.

[66] K. Suzuki, J. Sumitani, Y.W. Nam, T. Nishimaki, S. Tani, T. Wakagi, T. Kawaguchi, S. Fushinobu, Crystal structures of glycoside hydrolase family 3 β-glucosidase 1 from *Aspergillus aculeatus*, J. Biosci. Bioeng. 120 (2015) 614-623.

Table 1 Purification of BGLA.

Purification step	Total activity (U)[a]	Total protein (mg)[b]	Specific activity (U/mg)	Purification (fold)
Culture filtrate	5354.4	1983.1	2.7	1.0
$(NH_4)_2SO_4$ precipitation	4493.3	59.2	75.9	28.1
Toyopearl Super Q-650M	196.7	0.7	281.0	104.1

[a:] Activity was measured in citric acid/phosphate (pH 5.0) at 70°C using 3 mM p-Nitrophenyl-β-D-glucopyranoside (pNPG) as the substrate.

[b:] The protein content was assayed using a BCA Protein Assay Kit with bovine serum albumin as the standard.

Table 2 Substrate specificity of BGLA.

Substrate [a]	Specific activity (U/mg)
pNPG	73.56±0.87
Salicin	7.40±0.28
Cellobiose	6.50±0.30
Arbutin	12.97±0.59
Geniposide	6.11±0.07
Polydatin	4.91±0.16

[a]The specific activities were determined by measuring the amount of released p-nitrophenol (p-Nitrophenyl-β-D-glucopyranoside), glucose (salicin, cellobiose, arbutin and geniposide), or resveratrol (polydatin) after incubating them with the BGLA for 20 min at 70 °C, pH 5.0.

Figure captions

Fig. 1. SDS–PAGE analysis of BGLA. Lane M, protein molecular mass marker; lane 1, culture supernatant of *P. pastoris* transformed with pPIC9K empty vector control; lane 2, purified BGLA; lane 3, purified BGLA de-glycosylated using PNGase F.

Fig. 2. Effects of temperature and pH on the enzymatic activity and stability of BGLA. (A) Optimal temperature, the maximum activity obtained was defined as 100%; (B) Thermostability, the initial activity obtained was defined as 100%; (C) Optimal pH, the maximum activity obtained was defined as 100%; (D) pH stability, the initial activity obtained was defined as 100%. The results represent the means, and the error bars represent the SE based on three independent experiments.

Fig. 3. The effect of various metal ions on the enzymatic activity of BGLA. The activity of the enzyme in the absence of any additives was considered as the positive control (100%). The results represent the means, and the error bars represent the SE based on three independent experiments.

Fig. 4. (A) Root mean square deviation (RMSD) of the Cα atoms and (B) radius of gyration (Rg) of the whole BGLA as a function of time for the MD simulations at pH 5.0 and 2.0.

Fig. 5. (A) Contact number, (B) solvent accessible surface area (SASA) and (C) the number of hydrogen bonds (H-bonds) of the whole BGLA as a function of time for the MD simulations at pH 5.0 and 2.0.

Fig. 6. The values of root mean square fluctuation (RMSF) as a function of amino acid sequence at pH 2.0 and 5.0 during the 50-ns MD simulations.

Fig. 7. Representative structures of BGLA during the 50 ns of MD simulations at pH 2.0 (A) and pH 5.0 (B). The main chain of the protein is shown as a cartoon model. β-Sheets, α-helices, coils and loops are shown in yellow, purple, white, and blue, respectively. All the structures were rendered using the visual molecular dynamics (VMD) software (http://www.ks.uiuc.edu/Research/vmd/).

Fig. 8. The changes of distances between the residues Glu509 and Asp280 involved in the active site of BGLA during 50 ns of MD simulation.

Fig. 9. Representative conformations of the residues Glu509 and Asp280, which are involved in the active site of BGLA, at pH 2.0 (A) and pH 5.0 (B).

Fig. 1

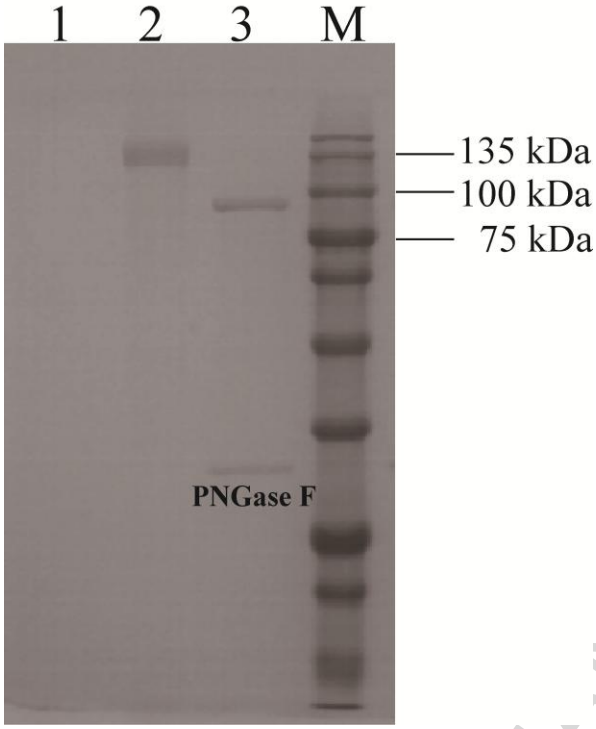

Fig. 2

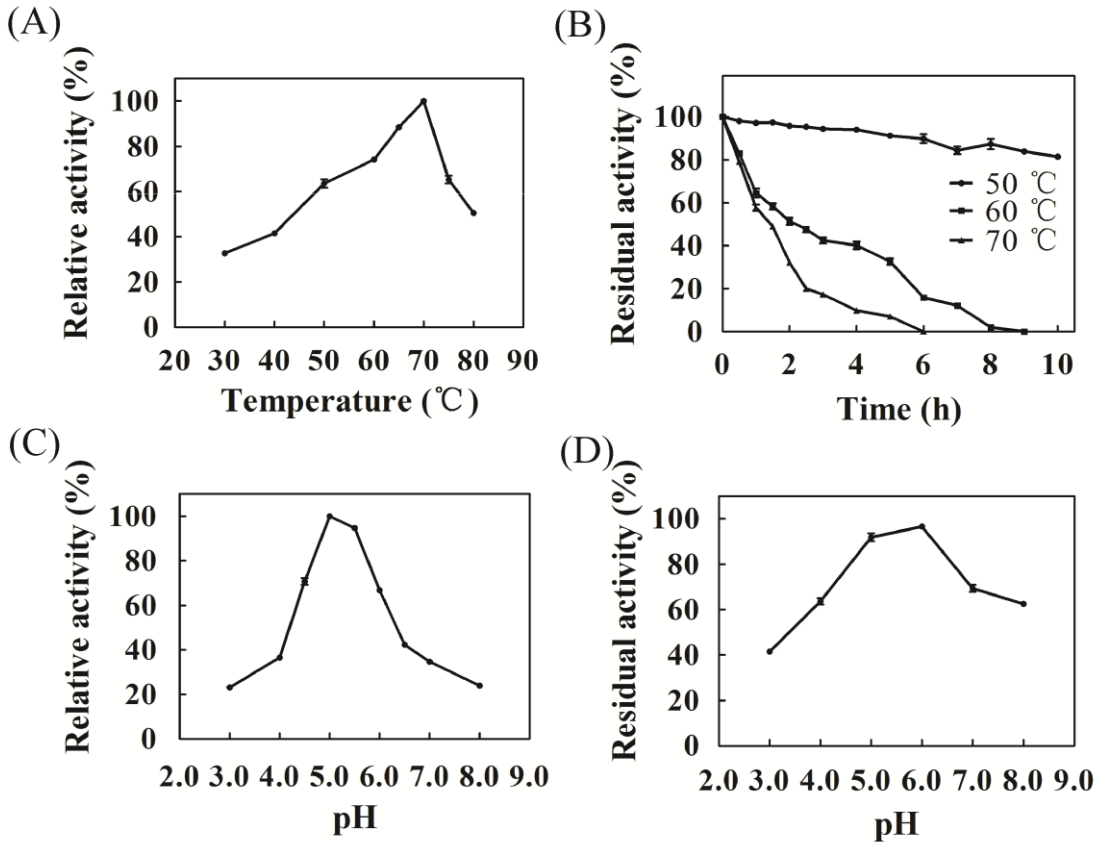

Fig. 3

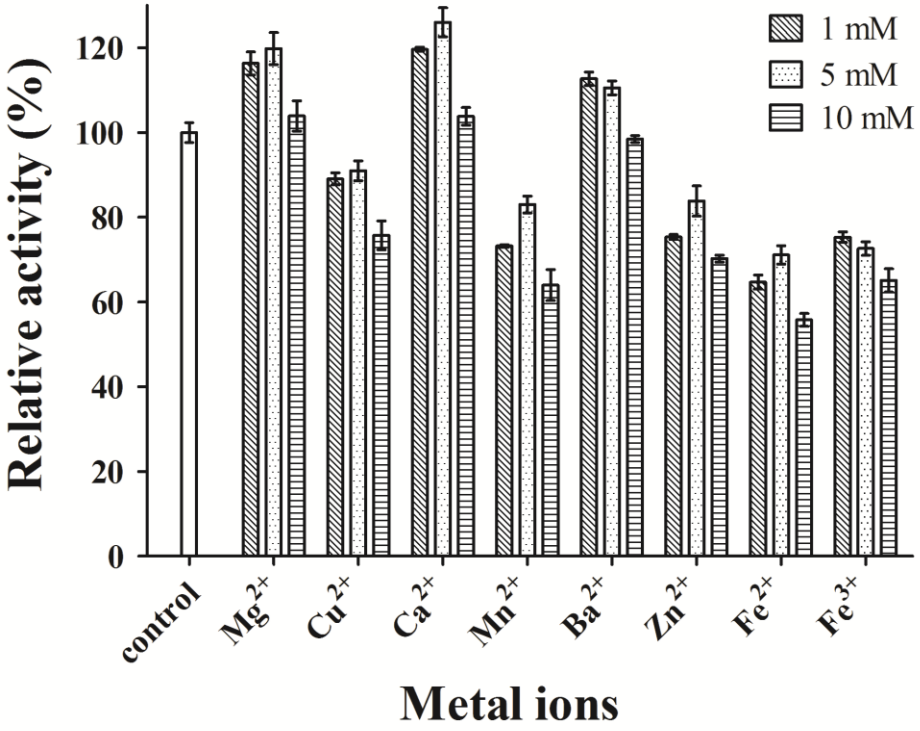

Fig. 4

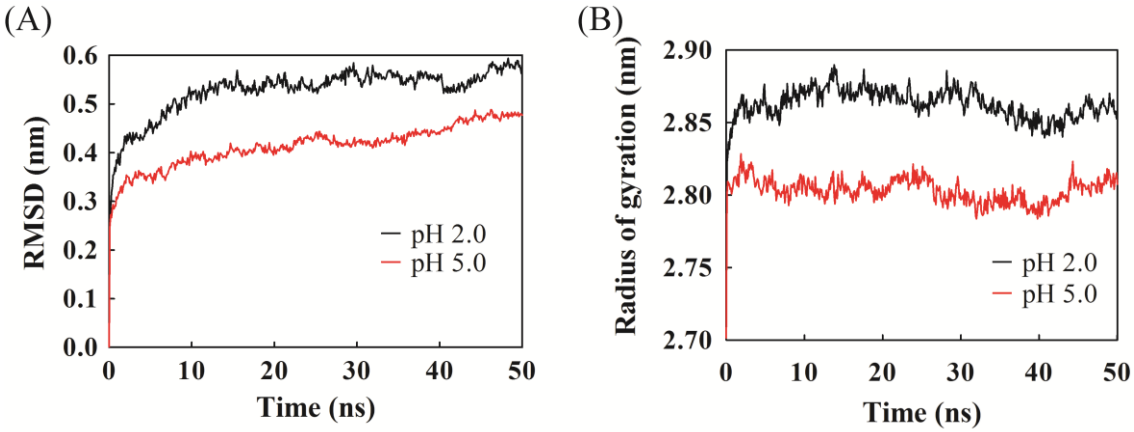

Fig. 5

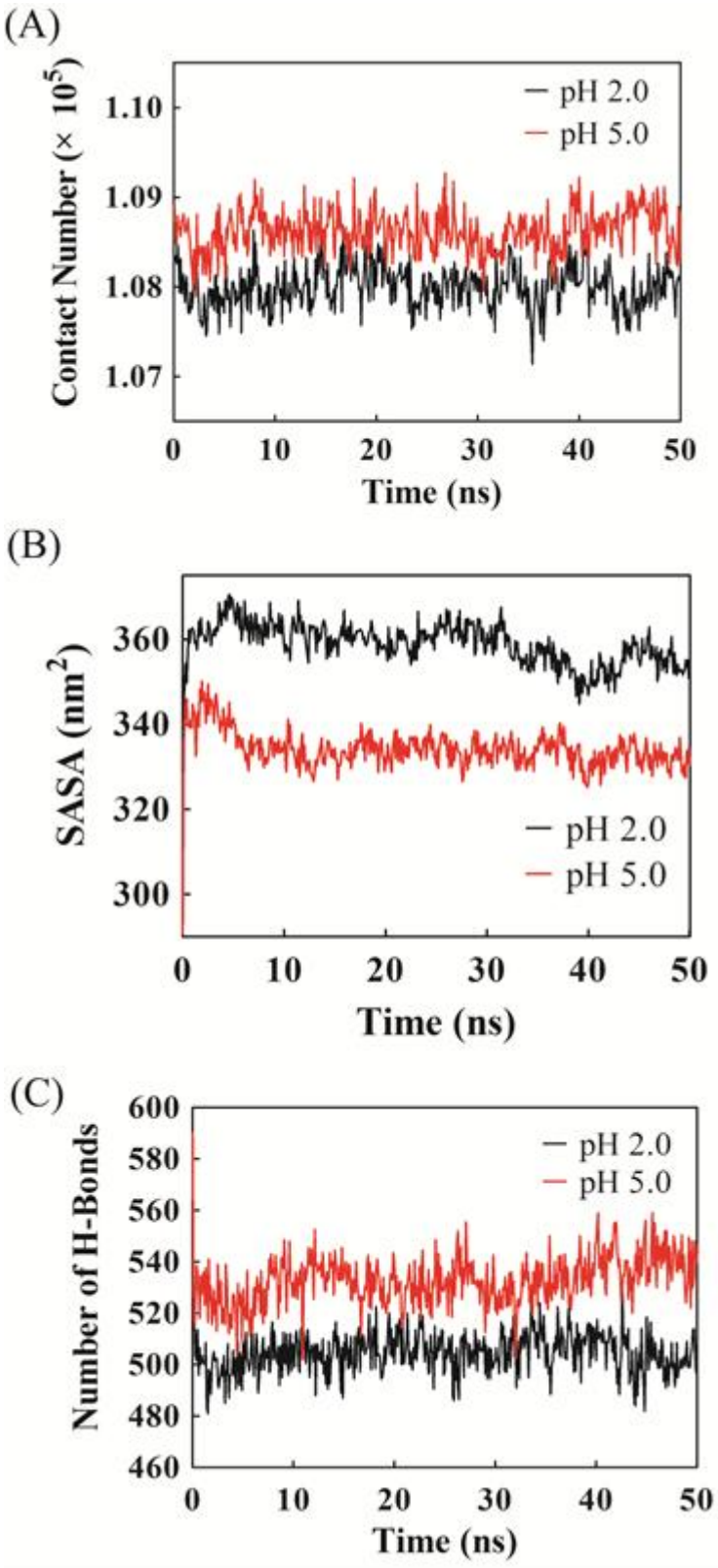

Fig. 6

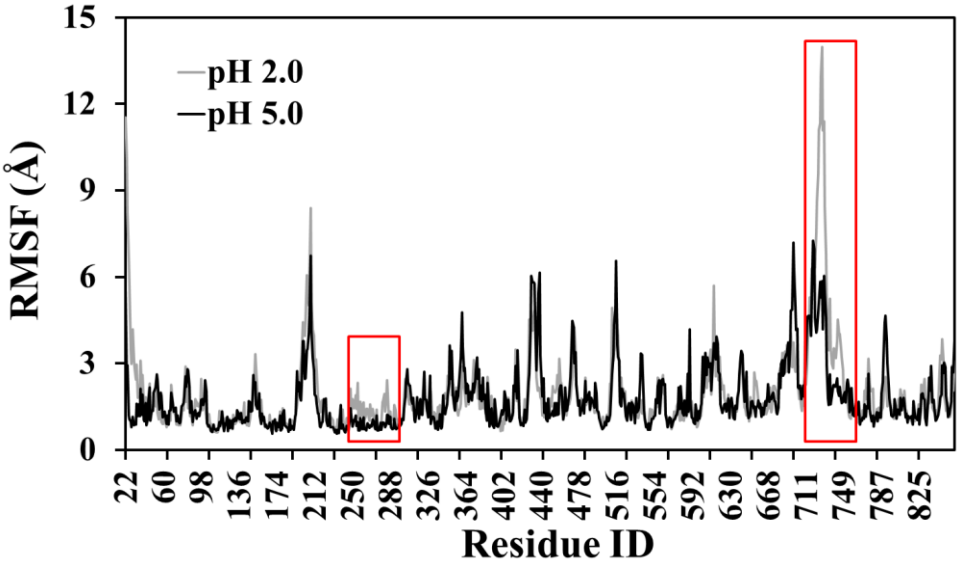

Fig. 7

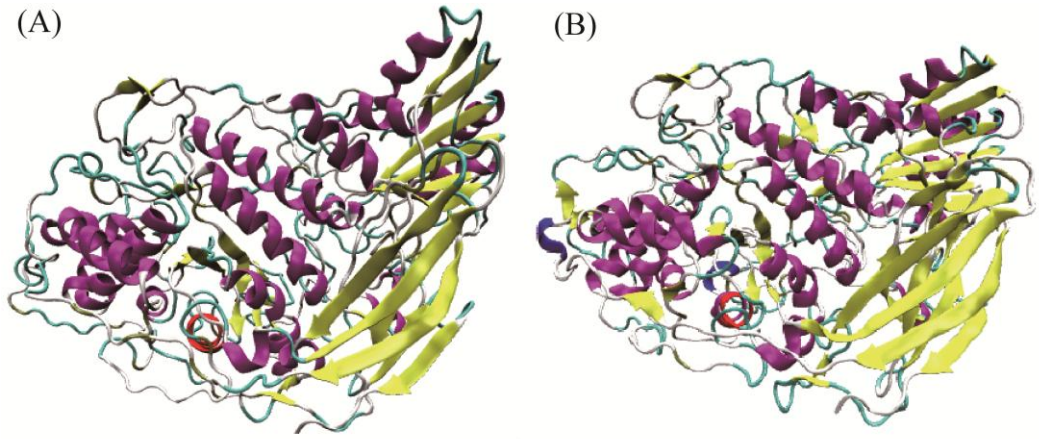

Fig. 8

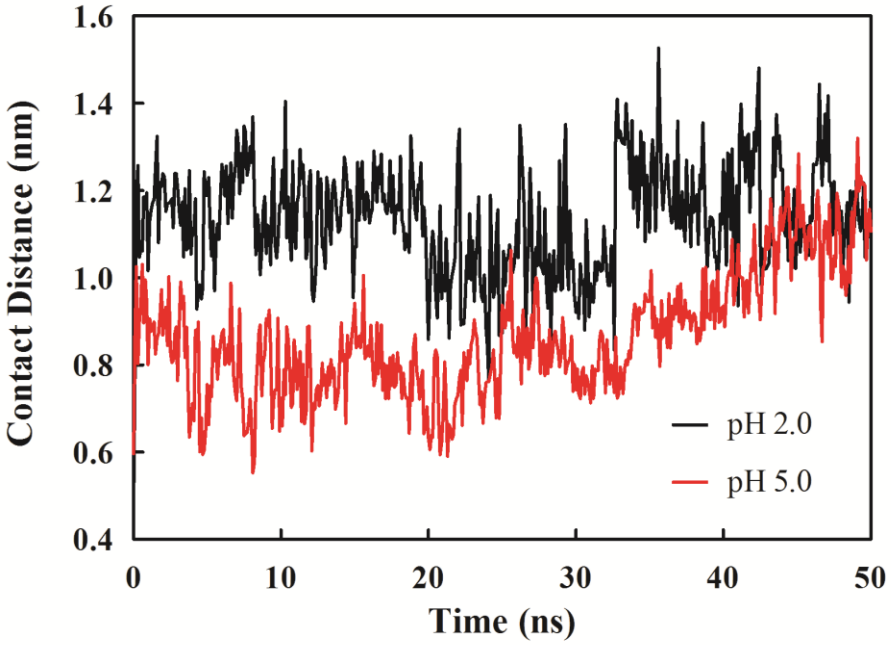

Fig. 9